Published in final edited form as:
J Immunol. 2013 March 15; 190(6): 2659–2669. doi:10.4049/jimmunol.1202531.

The Tec kinase ITK regulates thymic expansion, emigration, and maturation of γδ NKT cells[1]

Catherine C. Yin, **Ok Hyun Cho**, **Katelyn E. Sylvia**, **Kavitha Narayan**, **Amanda L. Prince**, **John W. Evans**, **Joonsoo Kang**, and **Leslie J. Berg**
Dept. of Pathology, University of Massachusetts Medical School, Worcester, MA 01655 USA

Abstract

The Tec family tyrosine kinase, Itk, regulates signaling downstream of the T cell receptor (TCR). The absence of Itk in $CD4^+$ T cells results in impaired Th2 responses along with defects in maturation, cytokine production and survival of *i*NKT cells. Paradoxically, $Itk^{-/-}$ mice have spontaneously elevated serum IgE levels, resulting from an expansion of the $V\gamma1.1^+V\delta6.3^+$ subset of γδ T cells, known as γδ NKT cells. Comparisons between γδ NKT cells and αβ *i*NKT cells showed convergence in the pattern of cell surface marker expression, cytokine profiles, and gene expression, suggesting that these two subsets of NKT cells undergo similar differentiation programs. Hepatic γδ NKT cells have an invariant TCR and are derived predominantly from fetal progenitors that expand in the thymus during the first weeks of life. The adult thymus contains these invariant γδ NKT cells plus a heterogeneous population of $V\gamma1.1^+V\delta6.3^+$ T cells with diverse CDR3 sequences. This latter population, normally excluded from the liver, escapes the thymus and homes to the liver when Itk is absent. In addition, $Itk^{-/-}$ γδ NKT cells persistently express high levels of *Zbtb16* (PLZF) and *Il4*, genes that are normally down-regulated in the most mature subsets of NKT cells. These data indicate that Itk signaling is required to prevent the expansion of γδ NKT cells in the adult thymus, to block their emigration, and to promote terminal NKT cell maturation.

Introduction

The Tec family tyrosine kinase, Itk, regulates signal transduction in T cells via the T-cell receptor (TCR). In the absence of Itk, T cells have defects in phospholipase C-γ1 (PLCγ1) activation, calcium mobilization, mitogen-activated protein kinase (MAPK kinase) phosphorylation, and AP-1 and nuclear factor of activated T cells (NFAT) activation following stimulation (1). As a consequence, Itk plays a critical role in αβ T cell development, influencing both positive and negative selection. During thymic development, conventional $CD4^+$ and $CD8^+$ T cells are the predominant populations that arise. These cells develop with a naïve phenotype ($CD62L^{hi}/CD44^{lo}$) and require a lengthy process of activation, proliferation, and differentiation prior to exhibiting effector cell characteristics (2–5). In contrast, thymic development in $Itk^{-/-}$ mice produces populations of both $CD4^+$ and $CD8^+$ T cells that resemble memory cells and exhibit innate effector functions (6–9). Thus, TCR signaling via Itk does not simply regulate the efficiency of conventional $CD4^+$ and $CD8^+$ T cell maturation, but also maintains the appropriate balance of naïve versus innate T cell subsets.

[1]Supported by NIH grants AI084987 and AI083505 to LJB and CA100382 to JK. The ImmGen Project is supported by a grant from the NIH (AI072073). Core resources supported by the Diabetes Endocrinology Research Center (DK32520) were also used.

Corresponding Author: Leslie J. Berg, Dept. Pathology, 55 Lake Ave No, Worcester, MA 01655 USA; phone: (508) 856-8371; leslie.berg@umassmed.edu.

One unexpected phenotype observed in *Itk*$^{-/-}$ mice was the spontaneous elevation in levels of serum IgE (10, 11). Based on data that indicated that *Itk*$^{-/-}$ conventional CD4^{+} T cells were unable to generate Th2 effector responses (12), and the fact that *Itk*$^{-/-}$ αβ TCR^{+} *i*NKT (αβ *i*NKT) cells were also defective in producing IL-4 (13, 14), the source of type 2 cytokines responsible for promoting B cell isotype switching to IgE was initially unclear. However, recent studies showed that the hyper-IgE syndrome seen in *Itk*$^{-/-}$ mice was dependent on γδ TCR^{+} T cells (15). Subset analysis of γδ T cells in *Itk*$^{-/-}$ mice identified the Vγ1.1^{+}Vδ6.3^{+} subset, expressing the transcription factor PLZF (hereafter referred to as V6 or γδ NKT cells) (16–18), as greatly increased in number in *Itk*$^{-/-}$ mice. Functional studies showed that these cells secreted high levels of Th2 cytokines (15). In addition to the shared expression of PLZF linking γδ to αβ NKT cells (19, 20), transcriptome analysis substantiated a common molecular program among these two cell lineages (21).

Elegant studies have demonstrated that the adult thymus contains a mixed population of γδ NKT cells. One subpopulation originates from fetal progenitors, undergoes substantial expansion in early neonatal life, and localizes to the liver; these cells predominantly express an invariant TCR sequence that is characterized by the absence of junctional diversity, consistent with their fetal/neonatal origin. In contrast, a second subpopulation is derived from adult precursors, and remains as a largely thymic resident population (22–24).

αβ *i*NKT cells are an innate subset of αβ T cells that reside in the thymus, spleen and liver, are rapid producers of cytokines such as IFNγ, IL-4, and IL-10 (25, 26), and predominantly express an invariant TCR (27). αβ *i*NKT cells develop in the thymus from CD4^{+}CD8^{+} double positive (DP) precursors, and are dependent on the presence of the nonclassical MHC class I molecule, CD1d (28–30). Following their initial positive selection, αβ *i*NKT cell precursors undergo additional stages of differentiation in the thymus. Starting with the earliest detectable population (CD24 (HSA)$^{+}$, TCR^{+}CD44^{lo}NK1.1^{lo}; stage 0), αβ *i*NKT cells proceed to down-regulate CD24 (stage 1), and then up-regulate CD44 (CD24^{lo}CD44^{hi}NK1.1^{lo}; stage 2). Finally, at the terminal maturation stage, the cells up-regulate the IL-2/IL-15 receptor β-chain (CD122) and NK cell receptors, such as NK1.1 (CD24^{lo}CD44^{hi}NK1.1^{hi}; stage 3). Transition through these stages is also accompanied by a change in cytokine profile. At the intermediate stage, αβ *i*NKT cells are potent producers of IL-4, but make little IFNγ; this phenotype correlates with expression of high levels of PLZF. As they transition to stage 3, αβ *i*NKT cells produce abundant amounts of IFNγ, but less IL-4, and PLZF expression decreases (31).

Previous studies have shown that *Itk*$^{-/-}$ mice have reduced numbers of αβ *i*NKT cells, and that those present have a defect in maturation (13, 14, 32). Although γδ T cells develop in the thymus, they develop from CD4^{-}CD8^{-} progenitors rather than from CD4^{+}CD8^{+} DP thymocytes (22, 33, 34), and their thymic selection requirements are not known. Thus, the exact extent of overlap in γδ and αβ *i*NKT cell developmental programs, and the impact of TCR signaling in γδ NKT cell differentiation are unclear. Here we show that CD24^{lo} γδ NKT thymocytes follow a maturational sequence composed of the three stages ascribed to αβ *i*NKT cells. *Itk*$^{-/-}$ γδ NKT cells are impaired in their maturation, leading to increased export of PLZF^{hi} IL-4-producing γδ NKT cells from the thymus. TCRδ sequence analysis indicated that, unlike the γδ NKT cells in livers of wild-type mice that are exclusively derived from fetal progenitors, *Itk*$^{-/-}$ hepatic γδ NKT cells include a subset derived from adult progenitors. These data indicate that Itk normally functions to prevent the expansion, as well as the export, of adult-origin γδ NKT cells, and that Itk plays a parallel role in the functional and phenotypic maturation of αβ and γδ NKT cells.

Material and Methods

Mice

Itk$^{-/-}$ mice (35) are on the C57BL/6 strain. 4Get mice (36) were crossed to *Itk*$^{-/-}$ mice to obtain *Itk*$^{-/-}$-4Get mice. *MHC2*$^{-/-}$ and β*2m*$^{-/-}$ mice were obtained from Jackson Labs or Taconic labs and are on a C57BL/6 background.s C57BL/6 mice were used as controls. Mice were used between 2–3 months of age and were maintained at the University of Massachusetts Medical School under specific pathogen-free conditions in accordance with institutional animal care and use committee guidelines.

Cell Preparations, Antibodies, and Flow Cytometry

To isolate lymphocytes from the liver, livers were first perfused with 5 ml PBS through the portal vein followed by collagenase digestion of minced liver. Lymphocytes were then isolated by Percoll gradient centrifugation. The following antibodies were purchased from BD Pharmingen: Rat anti-Mouse IgG1-FITC, Vδ6.2/6.3-PE, CD49a-AlexaFluor 647, IFNγ-AlexaFluor 700, and Ly49F-biotin (bio). NKG2A/C/E-FITC, TCRδ-PE-Cy5, TCRδ-PerCp eFluor 710, CD122-PerCp eFluor 710, IL-4-PE-Cy7, Streptavidin (Strep)-PE-Cy7, CD49a-Alexa Fluor 647, CD244.2-Alexa Fluor 647, TCRβ-allophycocyanin eFluor 780, CD24-eFluor 450 were purchased from e-Bioscience. CD8α-PE-Texas Red was purchased from Invitrogen Molecular Probes. CD1d-PBS57-PE and CD1d-PBS57 allophycocyanin tetramers were provided by the National Institute of Allergy and Infectious Diseases Tetramer Facility. Vγ1.1 antibody was a gift from Lynn Puddington (University of Connecticut Health Center, Farmington, CT) and conjugated to Alexa Fluor 647 with the Invitrogen Molecular Probes Alexa Fluor 647 Protein Labeling kit, or to biotin with FluoReporter Mini-Biotin-XX Protein Lableing kit also from Invitrogen Molecular Probes. Vγ1.1-FITC was purchased from BioLegend. The following antibodies were purchased from Santa Cruz Biotechnologies: PLZF (D-9) and normal mouse IgG. Cells (1×10^6–4×10^6 events) were collected on a LSRII (BD Biosciences) flow cytometer. Data were analyzed using FlowJo software (Tree Star).

In vitro T cell activation

WT and *Itk*$^{-/-}$ thymocytes were stimulated as previously described (15). Cells were surface stained for anti-TCRδ, anti-Vγ1.1$^+$, anti-Vδ6.3$^+$ or CD1d-PBS57 tetramer, fixed and permeabilized using fixation/permeabilization kit (e-Bioscience) and stained for IL-4, IFNγ and PLZF.

Sample Preparation for Microarray analysis

Samples were prepared for microarray analysis as described previously (21). Briefly, thymocytes were pooled from 4–30 mice and enriched for γδ T cells by depletion of CD8$^+$ cells with magnetic beads and an autoMACS. Cells were then stained and sorted with a FACSAria (~2×10^4 to 3×10^4 cells; >99% pure) directly into TRIzol (Invitrogen). Independent triplicates were sorted unless indicated otherwise (complete sorting details available from the ImmGen Project). Population labels correlate with ImmGen (immgen.org) populations as follows: mature WT thymic V6 (MatV6.WT), T.gd.vg1+vd6+24alo.Th; total V6 cells from *Itk*$^{-/-}$ thymus (TotalV6. *Itk*$^{-/-}$), T.gd.vg1+vd6+.Th.ITKko; mature WT CD4$^+$CD8$^-$ thymocytes (MatCD4), T.4SP24-.Th; mature WT CD4$^-$CD8$^+$ thymocytes (MatCD8), T.8SP24-.Th; WT thymic stage 0–1 *i*NKT cells (NKT.44$^-$NK1.1$^-$ (sorted in duplicate)), NKT.44-NK1.1-.Th; WT thymic stage 2 *i*NKT cells (NKT.44$^+$NK1.1$^-$), NKT.44+NK1.1-.Th; WT thymic stage 3 *i*NKT cells (NKT.44$^+$NK1.1$^+$), NKT.44+NK1.1+.Th. Note that all V6 cells in *Itk*$^{-/-}$ mice are CD24^{lo}.

Microarray data are available on the GEO website (www.ncbi.nlm.nih.gov/geo), accession #GSE15907.

Tcrd Cloning and Sequencing

Total RNA was isolated from WT and *Itk*$^{-/-}$ Vγ1.1^{+}Vδ6.3^{+} liver $\gamma\delta$ T cells. RNA was also isolated from WT-4Get and *Itk*$^{-/-}$-4Get mature (HSA^{lo}) Vγ1.1^{+}Vδ6.3^{+} thymic $\gamma\delta$ T cells that were GFP^{+}CD122^{-}, GFP^{+}CD122^{+} and GFP^{-}CD122^{+}. Reverse transcription (RT) of 0.2 μg RNA was performed with qScript DNA Supermix (Quanta™). TCRδ V region sequences were amplified from cDNA by PCR using published primers (37). Amplified sequences were cloned into pCR2.1®-TOPO® TA vector by TOPO® TA cloning kit (Invitrogen), and independent clones were subjected to DNA sequencing using both forward and reverse primers. To reduce sequencing error, only sequences confirmed in both directions were included in the alignment analysis. Additionally, rearrangements that resulted in out-of-frame junctions were also excluded from the final data set.

Data analysis and visualization

Two-tailed nonparametric Mann-Whitney tests were performed using Prism (Graph Pad software). Cell preparation and sorting for microarray analysis were performed as previously described by ImmGen standard operating procedures; see (21), Supplementary Notes 1 and 2. RNA processing and microarray analysis with the Affymetrix MoGene 1.0 ST array was performed at the ImmGen processing center (by ImmGen standard operating procedures; http://www.immgen.org/Protocols/ImmGen). Microarray data were analyzed and visualized as described previously (21). Briefly, data were analyzed with modules of the GenePattern genomic analysis platform. ConsolidatedProbeSets, a custom GenePattern module written by S. Davis (Harvard Medical School), was used for the consolidation of multiple probe sets into a single mean probe-set value for each gene. Genes with differences in regulation were identified with the Multiplot module of GenePattern through the use of the average of all replicates. Genes were considered to be regulated differently if they differed in expression by more than twofold, had a coefficient of variation among replicates of less than 0.5, had a Student's *t*-test *P* value of less than 0.05, and had a mean expression value of more than 120 in at least one subset in the comparison. Heat maps were generated by hierarchical clustering (HierarchicalClustering module of GenePattern) of data on the basis of gene (row) and subset (column) with the Pearson correlation for distance measurement. Data were log transformed and clustered with pairwise complete linkage. Data were centered on rows before visualization with the HeatMapViewer module of GenePattern. KEGG pathway analysis (Kyoto Encyclopedia of Genes and Genomes) was used for functional classifications through the DAVID portal.

Results

γδ NKT cells in the spleens of *Itk*$^{-/-}$ mice display an immature phenotype

We have previously shown that the absolute number and proportion of peripheral $\gamma\delta$T cells are increased in *Itk*$^{-/-}$ mice. This defect can be attributed to a specific subset of $\gamma\delta$T cells expressing the Vγ1.1^{+}Vδ6.3^{+} TCR (hereafter referred to as V6) (15) (Figure 1A). As numerous similarities between V6 cells and $\alpha\beta$ *i*NKT cells have been observed, we performed a side-by-side comparison of $\alpha\beta$ *i*NKT cells and V6 cells in the spleens of both WT and *Itk*$^{-/-}$ mice. Consistent with previous reports, $\alpha\beta$ *i*NKT cells from *Itk*$^{-/-}$ mice were reduced approximately two fold in both numbers and percentages (13, 14, 32). To focus on the later stages of NKT cell maturation, we analyzed CD24^{lo} subsets of V6 cells and $\alpha\beta$ *i*NKT cells, and found that the majority of these cells expressed the maturation markers CD44 and CD122. Furthermore, as described previously for $\alpha\beta$ *i*NKT cells (19, 20), maturation of WT V6 cells is associated with down-regulation of CD4 and PLZF (Figure

1B). Examination of the CD24^{lo} V6 population from *Itk*$^{-/-}$ mice revealed a drastically altered phenotype when compared to WT controls. While the majority of *Itk*$^{-/-}$ V6 cells expressed CD44 and CD122, similar to WT cells, they also aberrantly retained expression of PLZF and CD4, indicating incomplete maturation (Figure 1B). A similar trend, although less dramatic, was observed when comparing WT versus *Itk*$^{-/-}$ *i*NKT cells in the spleen, as reported previously, including modestly impaired up-regulation of CD122 and down-regulation of CD4 on *Itk*$^{-/-}$ *i*NKT cells (14).

To address the potential of these cells to produce cytokine, we first utilized IL-4 reporter mice (4Get; (36)), which express GFP from a bicistronic IL-4 mRNA. For these experiments, we compared the proportion of V6 and *i*NKT cells expressing GFP in the presence or absence of Itk. As shown in Figure 1C, the vast majority of V6 cells from the spleens of *Itk*$^{-/-}$ mice were GFP^{+}, compared to V6 cells from WT controls. Furthermore, the cell surface phenotype of GFP^{+} V6 cells from 4Get mice correlated with that of PLZF-expressing V6 cells, in both WT and *Itk*$^{-/-}$ mice (Figures 1B and C). Interestingly, analysis of 4Get mice showed that the *Itk*$^{-/-}$ *i*NKT cell population included fewer cytokine-producing cells than the WT *i*NKT cell subset, again consistent with previous published data (13, 14, 32). Taken together, these data indicate that majority of V6 cells from the spleens of *Itk*$^{-/-}$ mice display a more immature phenotype than their WT counterparts, a phenotype shared with *Itk*$^{-/-}$ *i*NKT cells.

Increased proportions of PLZF- and CD4-expressing γδ NKT cells in the livers of *Itk*$^{-/-}$ mice

Unlike conventional T cells, NKT cells preferentially home to the spleen and liver following thymic egress; furthermore, αβ *i*NKT cells continue to mature in the liver relative to their phenotype in the spleen (38). To determine whether a similar change was occurring with V6 cells, and whether *Itk*$^{-/-}$ liver V6 cells were also impaired in this maturation, we examined liver NKT cells. As shown in Figure 2, we found that fewer WT αβ *i*NKT cells and WT V6 cells in the liver expressed high levels of PLZF compared to these populations in the spleen (Figures 1B and 2A). A comparison of WT liver cells with those from *Itk*$^{-/-}$ mice showed that iNKT cells were similar; in contrast, *Itk*$^{-/-}$ liver V6 cells had a substantial increase in the proportion that expressed PLZF and CD4 (Figure 2A). Consistent with these data, an increased proportion of *Itk*$^{-/-}$ liver V6 cells also constitutively-expressed IL-4 mRNA (Figure 2B).

These data suggested that peripheral γδ NKT cell maturation was impaired in *Itk*$^{-/-}$ mice. Alternatively, we considered the possibility that adult *Itk*$^{-/-}$ mice might be generating unusually large numbers of PLZF^{+} V6 cells in the thymus, and that ongoing emigration of these cells was contributing substantially to the V6 population in the liver. This is in contrast to what is seen in WT mice, where the V6 cells found in the adult liver are predominantly derived from fetal/neonatal progenitors (22, 39). To address this latter possibility, we first examined the rearranged TCRδ gene sequences in V6 cells from the livers of WT and *Itk*$^{-/-}$ mice. As expected, liver V6 cells from WT mice exhibited extremely limited diversity in their TCRδ sequences, with 100% of the sequences identical to the canonical sequences previously found in V6 cells isolated from the fetal thymus, and distinguished by their absence of the Dδ1 and N region nucleotides (22). In contrast, TCRδ sequences from *Itk*$^{-/-}$ liver V6 cells included a fraction of sequences that were clearly of adult origin, in addition to those with the canonical TCRδ chain rearrangements (Figures 2C and S1). These data indicate that, in the absence of Itk, adult-derived thymic V6 cells are able to emigrate to the liver.

Altered thymic development of γδ NKT cells in *Itk*$^{-/-}$ mice

To address the changes in V6 cell development that might account for the presence of adult-derived γδ NKT cells in the liver of *Itk*$^{-/-}$ mice, we examined thymocytes from WT and *Itk*$^{-/-}$ mice, and characterized *i*NKT cell and V6 cell populations. As observed previously, the percentage of thymic *i*NKT cells in *Itk*$^{-/-}$ mice was decreased compared to WT (Figure 3A) (13–15). In contrast, *Itk*$^{-/-}$ thymi contained a substantial increase in the proportion of γδ T cells, an increase that was largely accounted for by expanded numbers of V6 cells (Figure 3A).

Several stages of αβ *i*NKT cell differentiation have been characterized based on a variety of cell surface markers, cytokines, and transcription factors. One notable example is the up-regulation of CD44 and CD122, which indicate a transition to the terminal maturation stage (40, 41). Similar to αβ *i*NKT cells, HSA^{lo} V6 cells up-regulate CD44 while concurrently up-regulating CD122 (Figure 3B). Analysis of *Itk*$^{-/-}$ thymic V6 cells indicated modest changes in the percentages of CD44^{+} and CD122^{+} cells compared to WT V6 cells, leading to a reduction in the proportion of CD44^{+} *Itk*$^{-/-}$ V6 cells that had up-regulated CD122. One difference between αβ *i*NKT cells and V6 cells was the expression of CD4; whereas WT αβ *i*NKT cells remained largely CD4^{+} in the thymus as they mature, WT thymic V6 cells down-regulated CD4 coincident with the up-regulation of CD44 and CD122. Strikingly, the majority of V6 cells in the thymus of *Itk*$^{-/-}$ mice remained CD4^{+} (Figure 3B). Together, these data suggest that γδ NKT cells in *Itk*$^{-/-}$ mice have a modest defect in the transition to terminal maturation, similar to the impaired maturation seen with thymic *Itk*$^{-/-}$ *i*NKT cells (Figure 3B and (14)).

A major transcription factor important in the development of αβ *i*NKT cells is PLZF (19, 20). As reported, PLZF levels decline as αβ *i*NKT cells mature; thus, the *i*NKT cells expressing the highest levels of CD44 or CD122 express less PLZF than their less mature counterparts ((19, 20) and Figure 3B). A parallel pattern of expression was evident for thymic V6 cells (Figure 3B), as has also recently been reported (42). For V6 cells, those expressing the highest levels of PLZF expressed less CD44 and CD122 than the PLZF^{int} subset. As shown, we observed an overall increase in the total numbers of both PLZF^{hi} and PLZF^{int} V6 populations among *Itk*$^{-/-}$ thymocytes (Figure 3D).

Another feature of αβ *i*NKT cell terminal maturation is a reduction in IL-4 production (32). To determine whether a similar pattern is observed for V6 cells, we analyzed thymocytes from WT- and *Itk*$^{-/-}$-4Get mice. V6 cells from WT mice showed graded GFP expression, such that the lowest levels of GFP correlated with the highest expression of maturation markers, CD44 and CD122. In addition, GFP-negative WT thymic V6 cells were also CD4-negative. *Itk*$^{-/-}$ thymic V6 cells showed a similar pattern; however, the proportion of cells retaining high levels of GFP was dramatically increased compared to WT (Figure 3C, D).

Cytokine production by γδ NKT cells correlates with PLZF expression

As αβ iNKT cells undergo terminal maturation, they switch from being single IL-4-producers to being dual producers of both IL-4 and IFNγ, a change that correlates with reduced PLZF expression (19, 20, 43). To determine whether V6 cells expressing high versus intermediate levels of PLZF showed a similar pattern of cytokine production, we stimulated WT and *Itk*$^{-/-}$ thymocytes with PMA and ionomycin and examined IFNγ and IL-4 production. Similar to αβ *i*NKT cells, V6 cells were capable of producing both cytokines upon stimulation, although the proportion of V6 cells producing IFNγ and IL-4 simultaneously is less than seen for αβ *i*NKT cells. Surprisingly, there was little difference in the frequency of total *Itk*$^{-/-}$ V6 cells capable of producing IFNγ and/or IL-4 compared to WT V6 cells (Figure 4A).

We then examined cytokine production in cells stained for PLZF expression. As can be seen in Figures 4B and 4C, only the PLZF^{int} subset of *i*NKT cells was capable of producing IFNγ, whereas both PLZF^{hi} and PLZF^{int} *i*NKT cells produced IL-4. A similar pattern was seen for V6 cells, and was shared between WT and *Itk*$^{-/-}$ thymocytes. These results indicate that PLZF^{hi} cells in *Itk*$^{-/-}$ mice are functionally competent, in spite of their delayed progression towards terminal maturation.

The gene signature of *Itk*$^{-/-}$ γδ NKT cells resembles immature WT *i*NKT cells

The data presented thus far suggest that the terminal maturation of V6 cells is impaired or delayed in the absence of Itk. To examine this issue at a molecular level, we performed gene expression microarray analysis. V6 cells were isolated from the thymus of *Itk*$^{-/-}$ mice, and their gene expression profile was compared to that of multiple populations of WT thymocytes. As shown in Figure 5, 71 genes were up-regulated by two-fold or more in *Itk*$^{-/-}$ V6 cells compared to WT CD24^{lo} V6 cells, and 124 genes were down-regulated (Figure 5A, Supp. Table 1). Using the Database for Annotation, Visualization and Integrated Discovery (DAVID) analysis program, we identified several KEGG (Kyoto Encyclopedia of Genes and Genomes) pathways that appeared to be dis-regulated in *Itk*$^{-/-}$ V6 cells (Figure 5B). These pathways were involved in cytokine signaling, some of which are required for the development of T cells, as well as effector functions, including molecules frequently associated with αβ *i*NKT and NK cells. To confirm these findings at the protein level, we examined the expression of several NK cell receptors that can mediate effector function in αβ *i*NKT cells. As shown, this analysis revealed that *Itk*$^{-/-}$ V6 cells have decreased or absent expression of CD122, NK1.1, 2B4, Ly49E/F, NKG2A/C/E, and CD94 compared to WT V6 cells (Figure 6A and B). As acquisition of NK cell receptors occurs at the final stage of αβ *i*NKT cell maturation (30, 32, 44), these data suggest that this developmental program is conserved for γδ NKT cells as well.

Given the similarity between αβ *i*NKT cells and V6 cells, we then examined the relationship between *Itk*$^{-/-}$ V6 cells and several isolated subsets of iNKT cells as well as conventional CD4 and CD8 thymocytes, using the αβ *i*NKT gene signature list generated previously (21). For this analysis, we compared the list of genes that were up-regulated in αβ *i*NKT cells versus naïve conventional CD4 and CD8 thymocytes, along with genes that were down-regulated in αβ *i*NKT cells versus CD4 and CD8 thymocytes, to the 124 genes that were down-regulated in *Itk*$^{-/-}$ V6 cells relative to WT V6 cells. Approximately 40% of the genes (51 genes) that were decreased in *Itk*$^{-/-}$ versus WT V6 cells are shared with the subset of genes normally up-regulated in αβ *i*NKT cells relative to conventional CD4 and CD8 T cells (Figure 5C). In contrast, only ~5% of the genes (6 genes) that were decreased in *Itk*$^{-/-}$ V6 cells are common to the genes normally down-regulated in αβ *i*NKT cells. These data indicate that the WT V6 cells are similar to WT αβ *i*NKT cells, and further, that *Itk*$^{-/-}$ V6 cells are lacking a subset of the mature αβ *i*NKT cell signature. Using cluster analysis and comparing the 51 genes that WT αβ *i*NKT and *Itk*$^{-/-}$ V6 cells share in Figure 5C, the heat map shows that WT HSA^{lo} V6 cells are similar to mature WT αβ *i*NKT cells while the *Itk*$^{-/-}$ V6 cells are most similar to immature (NK1.1^{-}) WT αβ *i*NKT cells (Figure 5D and Supp. Table 2). Together with the phenotypic analysis, these data confirm that *Itk*$^{-/-}$ V6 cells are impaired in their terminal maturation in the thymus.

Itk$^{-/-}$ thymic γδ NKT cells are derived from both fetal and adult progenitors

Previous studies have demonstrated that peripheral V6 cells in WT mice arise from fetal progenitors that expand in number in the neonatal thymus, and migrate out to populate peripheral tissues (22, 24). In contrast, the V6 cells found in adult *Itk*$^{-/-}$ liver included a subset that was clearly derived from adult progenitors. These findings suggested that Itk might be required to specifically limit the numbers of adult progenitor-derived V6 cells in

the thymus; for example, Itk might be required to promote a TCR-dependent cell death signal, akin to the negative selection of conventional T cells. If this were the case, we would predict that thymic V6 cells in adult *Itk*$^{-/-}$ mice would be greatly enriched for the adult progenitor-derived population. In addition, we considered the possibility that PLZF^{hi} versus PLZF$^{int/lo}$ V6 cells might represent distinct V6 subsets. For instance, it was possible that PLZF$^{int/lo}$ cells represented the continued presence of fetal progenitor-derived V6 cells expressing the invariant TCR delta sequence, whereas the PLZF^{hi} cells might represent V6 cells developing in the adult thymus from adult progenitors.

To address these issues, we analyzed three populations of V6 cells from the thymus of WT and *Itk*$^{-/-}$ mice. To facilitate the isolation of distinct subsets, we utilized WT-4Get and *Itk*$^{-/-}$-4Get thymocytes, and sorted GFP^{hi}CD122^{-} (stage 1), GFP^{int}CD122^{+} (stage 2), and GFP^{-}CD122^{+} (stage 3) populations, taking advantage of the fact that GFP expression is correlated with PLZF expression in V6 cells (see Figure 3). TCRδ sequence analysis indicated the presence of a highly diverse repertoire in each of the subsets, and in both WT and *Itk*$^{-/-}$ mice (Figure S1). Furthermore, a significant proportion of the sequences from both WT and *Itk*$^{-/-}$ thymocytes of each subset utilized Dδ1 and contained N region additions, indicating that these adult thymic V6 cells were not derived from fetal progenitors. Nonetheless, the invariant TCRδ sequence found in WT liver V6 cells was detected in each of the adult thymic V6 subsets, confirming the persistence of these fetal-derived cells in the adult thymus, as previously reported (22).

A detailed inspection of the data from WT thymocytes showed that, among the more mature V6 subsets (CD122^{+} stages 2 and 3), there was a reduced proportion of these fetal progenitor-derived sequences relative their abundance in the less mature GFP^{hi} CD122^{-} subset, stage 1 ($p<0.0001$ and $p=0.002$, respectively; Figure 7). This finding indicated selection against this invariant TCR during the maturation of adult thymic V6 cells. While overall the pattern of TCRδ sequences among adult thymic *Itk*$^{-/-}$ V6 cells was similar to that seen in the WT adult thymus, we did observe an apparent lack of selection against the invariant fetal progenitor-derived sequence as *Itk*$^{-/-}$ V6 cells mature. These data indicated that the numerical increase in V6 cells in the *Itk*$^{-/-}$ thymus was not due to a preferential expansion of adult progenitor-derived cells, but instead, was the result of expansion of both fetal- and adult-derived V6 cell subsets. Furthermore, these data demonstrated that, in the WT thymus, V6 subsets distinguished by high or low PLZF expression and/or CD122 expression were not derived from different progenitors; instead, each population contained a mixture of cells of both origins. As a result, these data support the conclusion that V6 stages 1→2→3 represent a developmental lineage of γδ NKT cells.

Discussion

In order to understand the basis for the γδ T cell-dependent hyper-IgE syndrome that develops in the absence of Itk, we performed a detailed analysis γδ NKT cells in *Itk*$^{-/-}$ mice. Our previous studies demonstrated that this γδ T cell subset, expressing the Vγ1.1/Vδ6.3 (V6) TCR and the transcription factor PLZF, was highly expanded in *Itk*$^{-/-}$ mice and could secrete large amounts of Type II cytokines, such as IL-4 and IL-13 (15). Using a combination of phenotypic, functional, and molecular analysis of V6 cells in the thymus, spleen, and liver, we have determined a number of important features of these cells. First, we show that the increased V6 population in *Itk*$^{-/-}$ mice is generally accounted for by cells expressing high levels of PLZF and constitutively-expressing IL-4 mRNA. Second, based on a comparison to *i*NKT cells, we conclude that *Itk*$^{-/-}$ V6 cells do not fully mature and cannot transit to the stage associated with high level IFNγ production. Third, we provide evidence that *Itk*$^{-/-}$ V6 cells arising from adult progenitors are migrating to the liver, a process that is not permitted for WT V6 cells. Together, these findings reveal alterations in the V6 γδ NKT

cell population present in *Itk*$^{-/-}$ mice that could account for the hyper-IgE syndrome seen in these mice.

We found a number of striking parallels between V6 cells and *i*NKT cells that suggest a common developmental program shared between these two cell lineages. Recently, we found that mature WT thymic V6 cells and thymic *i*NKT cells express a common NKT cell gene expression signature (21). By examining changes in cell surface marker expression, PLZF levels, and cytokine profiles, we now show that γδ NKT cells can be subdivided into populations nearly identical to the Stage1–3 subsets of *i*NKT cells (27, 41, 46). This comparison indicates that the most mature subset of V6 cells in the thymus are PLZF^{int}, express markers of activation (CD44, CD122, and a host of NK receptors), down-regulate CD4, and are dual producers of IFNγ and IL-4. Furthermore, our TCRδ sequence analysis showed that both IL-4^{+} PLZF^{hi} and IL-4/IFNγ^{+} PLZF^{int} subsets contain a mixture of invariant fetal-derived and heterogeneous adult-derived TCRδ gene rearrangements. This result supports a model of a common developmental program for these two γδ NKT cell subpopulations.

A major unresolved issue is the underlying cause of increased numbers of more immature PLZF^{hi} V6 cells in *Itk*$^{-/-}$ mice. One possibility is that competition exists between γδ NKT cells and αβ *i*NKT cells, and *Itk*$^{-/-}$ V6 cell numbers are increased due to a reduction in αβ *i*NKT cells in these mice. However, a recent study showed that this competition was acting on the most mature NK1.1^{+} PLZF^{lo} subset of each NKT cell population (14). As our data indicate that it is predominantly the NK receptor negative PLZF^{hi} population of γδ NKT cells that is increased in *Itk*$^{-/-}$ mice, it seems unlikely that the observed expansion is caused by a reduced number of *Itk*$^{-/-}$ αβ *i*NKT cells.

Instead, we suggest that the increased number of *Itk*$^{-/-}$ γδ NKT cells, as well as their impaired terminal maturation, is due to defective TCR signaling in the absence of Itk. For αβ *i*NKT cells, TCR signaling has been shown to be essential for their maturation to the NK1.1^{+} stage, as this developmental progression fails to occur in the absence of Zap-70 (45). For V6 cells, enforced Vγ1.1/Vδ6.3 TCR transgene enhanced the generation of PLZF^{+} NKT cells, indicating that TCR signaling provides a selective cue (16). While comprehensive analysis of progressive γδ NKT cell maturation in mice with mutations in TCR signaling components has not been performed, our data demonstrate that stage 1 V6 cells do not efficiently mature when Itk signaling is impaired. In aggregate, these findings support the hypothesis that qualitatively distinct TCR signaling occurs at multiple maturation checkpoints for both αβ and γδ NKT cells.

For γδ T cells, TCR-dependent maturation processes are not restricted to the NKT subset, as the maturation of other γδ T cell subsets has been shown to be modulated by TCR signaling. Studies of a natural population of nonclassical MHC class I T10/22-specific γδ T cells have revealed several interesting features of γδTCR signaling-mediated thymic selection processes. First, the presence of the cognate ligand for this γδ subset in WT C57Bl/6 mice reduces the numbers of T22 tetramer-binding cells, indicative of a negative selection process. Second, mice lacking T10/22 still generate the tetramer^{+} γδ T cells, but these cells are deficient in IFNγ production, whereas the tetramer^{+} cells found in WT mice are primarily IFNγ-producers. These data indicate that intrathymic TCR signaling promotes the generation of γδ effector cells fated for IFNγ production (46). Third, examination of the cell surface phenotype of γδ TCR^{+} thymocytes shows an inverse correlation between CD122 expression and expression of the gut-homing chemokine receptor, CCR9, such that cells expressing high levels of CD122 express little CCR9. Importantly, in mice lacking T10/T22, all T22 tetramer^{+} γδ TCR^{+} thymocytes express high levels of CCR9, whereas in WT mice expressing the self-ligand, a majority of these cells are CCR9^{-} and CD122^{+}. These

findings provide a clear precedent for intrathymic TCR signaling-mediated maturation of γδ T effector subsets, and support our conclusion that *Itk*$^{-/-}$ γδ NKT cells escape negative selection, do not efficiently up-regulate CD122 and fail to down-regulate CCR9, due to impaired TCR signaling. Our efforts to define a potential TCR-dependent ligand for V6 cells in the thymus have, to date, been largely unsuccessful. We find that V6 cells are not dependent on classical or nonclassical MHC Class I or Class II molecules for their development (Figure S2). Nonetheless, additional studies of genetically-modified mice support the conclusion that V6 cell development is strongly influenced by TCR signaling. Specifically, mice deficient for Kruppel-like factor 2 (KLF2) (47) or inhibitor of DNA binding 3 (Id3) (17, 48), as well as mice expressing a mutant form of the SLP-76 adapter protein (SLP76-Y145F) that is unable to bind to ITK (17, 49), have been analyzed. In each of these cases, the mice exhibit a similar phenotype to *Itk*$^{-/-}$ mice, characterized by a dramatic increase in the numbers of thymic V6 cells. Together, these data are consistent with the model that γδ NKT cells normally undergo negative selection due to robust TCR signaling in the thymus.

In the absence of Itk, adult thymic γδ NKT cells are able to emigrate from the thymus. It is also possible that the invariant fetal-derived V6 cells also continue to emigrate from the thymus in adult *Itk*$^{-/-}$ mice (Figure 8), although we cannot resolve this issue based on our current analysis. One possible explanation for the deregulation of V6 cell migration in the absence of Itk is a failure of *Itk*$^{-/-}$ V6 cells to down-regulate chemokine receptors that may promote T cell trafficking to peripheral organs. Consistent with this notion, our microarray data indicate that, in addition to CCR9, CCR2 is more highly expressed in *Itk*$^{-/-}$ V6 cells compared to WT controls. While CCR9 is one of the receptors that can induce homing to the gut as well as to other peripheral tissues, it is only modestly expressed on *i*NKT cells in the liver. In contrast, CCR2 is highly expressed in *i*NKT cells isolated from the liver, and interestingly, is most abundant in the CD4^{+} fraction of this population (www.immgen.org). These findings suggest that a failure to down-regulate CCR2 as adult thymic γδ NKT cells mature could account for their continued ability to emigrate from the thymus and home to the liver.

Our findings also clarify some of the inconsistent data regarding the development of V6 cells in *Id3*$^{-/-}$ and *Itk*$^{-/-}$ mice. Previous reports demonstrated that similar to *Itk*$^{-/-}$ mice, *Id3*$^{-/-}$ mice had an increase in V6 cells (17, 48). We previously showed that reconstitution of WT mice with *Itk*$^{-/-}$ bone marrow cells resulted in donor-specific generation of the expanded V6 population (15), whereas reconstitution of WT mice with *Id3*$^{-/-}$ bone marrow failed to do so (18). This difference might arise if the Id3-deficiency selectively affected the expansion of the fetal progenitor-derived V6 cell population, whereas the lack of Itk led to an expansion of both V6 cell populations. In support of this interpretation, analysis of TCRδ sequences among adult thymic V6 cells from *Id3*$^{-/-}$ mice indicates that 84% of the cells are derived from fetal progenitors, a substantially higher proportion than seen in the adult *Itk*$^{-/-}$ thymus (18).

Recently, *Lin28b* has been found to play an essential role in programming fetal liver and fetal thymic hematopoietic progenitor cells to generate unique subsets of innate-like B and T lymphocytes (50). In particular, mice transplanted with *Lin28b*-transduced adult bone marrow stem cells developed a greater than ten-fold increase in the numbers of PLZF^{+} αβ and γδ NKT cells relative to mice reconstituted with WT bone marrow cells. These important findings raise the formal possibility that Lin28b expression is dis-regulated in mice that show expanded populations of PLZF^{+} innate T cells, such as *Id3*$^{-/-}$ mice. In the case of *Itk*$^{-/-}$ mice, altered regulation of the *Lin28b* pathway is unlikely to fully account for the increased number of V6 cells in the adult *Itk*$^{-/-}$ thymus, as we see a concomitant decrease in the numbers of αβ *i*NKT cells. Thus, while there are likely distinct progenitor-

specific programs controlling fetal versus adult NKT cell differentiation, Itk-dependent TCR signaling is an arbiter of the size of NKT cell populations and is required for their terminal maturation.

Supplementary Material

Refer to Web version on PubMed Central for supplementary material.

Acknowledgments

We thank Regina Whitehead and Sharlene Hubbard for technical assistance. We also thank members of the ImmGen core team (M. Painter, J. Ericson and S. Davis) for help with data generation and processing; and eBioscience, Affymetrix and Expression Analysis for support of the ImmGen Project.

References

1. Andreotti AH, Schwartzberg PL, Joseph RE, Berg LJ. T-Cell Signaling Regulated by the Tec Family Kinase, Itk. Cold Spring Harbor Perspectives in Biology. 2010; 2:a002287–a002287. [PubMed: 20519342]
2. Kaech SM, Wherry EJ, Ahmed R. Effector and memory T-cell differentiation: implications for vaccine development. Nat. Rev. Immunol. 2002; 2:251–262. [PubMed: 12001996]
3. Surh CD, Sprent J. Regulation of mature T cell homeostasis. Seminars in Immunology. 2005; 17:183–191. [PubMed: 15826823]
4. Jameson SC. T cell homeostasis: keeping useful T cells alive and live T cells useful. Seminars in Immunology. 2005; 17:231–237. [PubMed: 15826828]
5. Smith-Garvin JE, Koretzky GA, Jordan MS. T Cell Activation. Annu. Rev. Immunol. 2009; 27:591–619. [PubMed: 19132916]
6. Atherly LO, Lucas JA, Felices M, Yin CC, Reiner SL, Berg LJ. The Tec family tyrosine kinases Itk and Rlk regulate the development of conventional CD8+ T cells. Immunity. 2006; 25:79–91. [PubMed: 16860759]
7. Broussard C, Fleischacker C, Fleischecker C, Horai R, Chetana M, Venegas AM, Sharp LL, Hedrick SM, Fowlkes BJ, Schwartzberg PL. Altered development of CD8+ T cell lineages in mice deficient for the Tec kinases Itk and Rlk. Immunity. 2006; 25:93–104. [PubMed: 16860760]
8. Dubois S, Waldmann TA, Müller JR. ITK and IL-15 support two distinct subsets of CD8+ T cells. Proc. Natl. Acad. Sci. U.S.A. 2006; 103:12075–12080. [PubMed: 16880398]
9. Hu J, August A. Naive and innate memory phenotype CD4+ T cells have different requirements for active Itk for their development. J. Immunol. 2008; 180:6544–6552. [PubMed: 18453573]
10. Mueller C, August A. Attenuation of immunological symptoms of allergic asthma in mice lacking the tyrosine kinase ITK. J. Immunol. 2003; 170:5056–5063. [PubMed: 12734350]
11. Schaeffer EM, Yap GS, Lewis CM, Czar MJ, McVicar DW, Cheever AW, Sher A, Schwartzberg PL. Mutation of Tec family kinases alters T helper cell differentiation. Nat Immunol. 2001; 2:1183–1188. [PubMed: 11702066]
12. Kosaka Y, Felices M, Berg LJ. Itk and Th2 responses: action but no reaction. Trends in Immunology. 2006; 27:453–460. [PubMed: 16931156]
13. Au-Yeung BB, Fowell DJ. A key role for Itk in both IFN gamma and IL-4 production by NKT cells. J. Immunol. 2007; 179:111–119. [PubMed: 17579028]
14. Felices M, Berg LJ. The Tec kinases Itk and Rlk regulate NKT cell maturation, cytokine production, and survival. J. Immunol. 2008; 180:3007–3018. [PubMed: 18292523]
15. Felices M, Yin CC, Kosaka Y, Kang J, Berg LJ. Tec kinase Itk in gammadeltaT cells is pivotal for controlling IgE production in vivo. Proceedings of the National Academy of Sciences. 2009; 106:8308–8313.
16. Kreslavsky T, Savage AK, Hobbs R, Gounari F, Bronson R, Pereira P, Pandolfi PP, Bendelac A, von Boehmer H. TCR-inducible PLZF transcription factor required for innate phenotype of a

subset of gammadelta T cells with restricted TCR diversity. Proceedings of the National Academy of Sciences. 2009; 106:12453–12458.

17. Alonzo ES, Gottschalk RA, Das J, Egawa T, Hobbs RM, Pandolfi PP, Pereira P, Nichols KE, Koretzky GA, Jordan MS, Sant'Angelo DB. Development of Promyelocytic Zinc Finger and ThPOK-Expressing Innate T Cells Is Controlled by Strength of TCR Signaling and Id3. J. Immunol. 2010; 184:1268–1279. [PubMed: 20038637]
18. Verykokakis M, Boos MD, Bendelac A, Adams EJ, Pereira P, Kee BL. Inhibitor of DNA Binding 3 Limits Development of Murine Slam-Associated Adaptor Protein-Dependent “Innate” γδ T cells. PLoS ONE. 2010; 5:e9303. [PubMed: 20174563]
19. Kovalovsky D, Uche OU, Eladad S, Hobbs RM, Yi W, Alonzo E, Chua K, Eidson M, Kim H–J, Im JS, Pandolfi PP, Sant'Angelo DB. The BTB-zinc finger transcriptional regulator PLZF controls the development of invariant natural killer T cell effector functions. Nat Immunol. 2008; 9:1055–1064. [PubMed: 18660811]
20. Savage AK, Constantinides MG, Han J, Picard D, Martin E, Li B, Lantz O, Bendelac A. The Transcription Factor PLZF Directs the Effector Program of the NKT Cell Lineage. Immunity. 2008; 29:391–403. [PubMed: 18703361]
21. Narayan K, Sylvia KE, Malhotra N, Yin CC, Martens G, Vallerskog T, Kornfeld H, Xiong N, Cohen NR, Brenner MB, Berg LJ, Kang J. Intrathymic programming of effector fates in three molecularly distinct gamma-delta T cell subtypes. Nat Immunol. 2012; 13:511–518. [PubMed: 22473038]
22. Grigoriadou K, Boucontet L, Pereira P. Most IL-4-producing gamma delta thymocytes of adult mice originate from fetal precursors. J. Immunol. 2003; 171:2413–2420. [PubMed: 12928388]
23. Gerber DJ, Azuara V, Levraud JP, Huang SY, Lembezat MP, Pereira P. IL-4-producing gamma delta T cells that express a very restricted TCR repertoire are preferentially localized in liver and spleen. J. Immunol. 1999; 163:3076–3082. [PubMed: 10477572]
24. Azuara V, Levraud JP, Lembezat MP, Pereira P. A novel subset of adult gamma delta thymocytes that secretes a distinct pattern of cytokines and expresses a very restricted T cell receptor repertoire. Eur. J. Immunol. 1997; 27:544–553. [PubMed: 9045929]
25. Kronenberg M. Toward an understanding of NKT cell biology: progress and paradoxes. Annu. Rev. Immunol. 2005; 23:877–900. [PubMed: 15771592]
26. Van Kaer L. Regulation of Immune Responses by CD1d-Restricted Natural Killer T Cells. Immunol Res. 2004; 30:139–154. [PubMed: 15477656]
27. Bendelac A, Savage PB, Teyton L. The Biology of NKT Cells. Annu. Rev. Immunol. 2007; 25:297–336. [PubMed: 17150027]
28. Bendelac A. Positive selection of mouse NK1+ T cells by CD1-expressing cortical thymocytes. J. Exp. Med. 1995; 182:2091–2096. [PubMed: 7500054]
29. Coles MC, Raulet DH. NK1.1+ T cells in the liver arise in the thymus and are selected by interactions with class I molecules on CD4+CD8+ cells. J. Immunol. 2000; 164:2412–2418. [PubMed: 10679077]
30. Gapin L, Matsuda JL, Surh CD, Kronenberg M. NKT cells derive from double-positive thymocytes that are positively selected by CD1d. Nat Immunol. 2001; 2:971–978. [PubMed: 11550008]
31. Prince AL, Yin CC, Enos ME, Felices M, Berg LJ. The Tec kinases Itk and Rlk regulate conventional versus innate T-cell development. Immunol. Rev. 2009; 228:115–131. [PubMed: 19290924]
32. Gadue P, Stein PL. NK T cell precursors exhibit differential cytokine regulation and require Itk for efficient maturation. J. Immunol. 2002; 169:2397–2406. [PubMed: 12193707]
33. Petri HT, Scollay R, Shortman K. Commitment to the T cell receptor αβ or γδ lineages can occur just prior to the onset of CD4 and CD8 expression among immature thymocytes. Eur. J. Immunol. 1992; 22:2185–2188. [PubMed: 1386319]
34. Kang J, Volkmann A, Raulet DH. Evidence that gammadelta versus alphabeta T cell fate determination is initiated independently of T cell receptor signaling. J. Exp. Med. 2001; 193:689–698. [PubMed: 11257136]

35. Liu KQ, Bunnell SC, Gurniak CB, Berg LJ. T cell receptor–initiated calcium release is uncoupled from capacitative calcium entry in Itk-deficient T cells. J. Exp. Med. 1998; 187:1721–1727. [PubMed: 9584150]
36. Mohrs M, Shinkai K, Mohrs K, Locksley RM. Analysis of type 2 immunity in vivo with a bicistronic IL-4 reporter. Immunity. 2001; 15:303–311. [PubMed: 11520464]
37. Aydintug MK, Roark CL, Yin X, Wands JM, Born WK, O'Brien RL. Detection of cell surface ligands for the gamma delta TCR using soluble TCRs. J. Immunol. 2004; 172:4167–4175. [PubMed: 15034029]
38. Pellicci DG, Hammond KJL, Uldrich AP, Baxter AG, Smyth MJ, Godfrey DI. A natural killer T (NKT) cell developmental pathway involving a thymus-dependent NK1. 1− CD4+ CD1d-dependent precursor stage. J. Exp. Med. 2002; 195:835–844. [PubMed: 11927628]
39. Gerber D, Boucontet L, Pereira P. Early expression of a functional TCRbeta chain inhibits TCRgamma gene rearrangements without altering the frequency of TCRgammadelta lineage cells. J. Immunol. 2004; 173:2516–2523. [PubMed: 15294967]
40. Godfrey DI, Berzins SP. Control points in NKT-cell development. Nat. Rev. Immunol. 2007; 7:505–518. [PubMed: 17589542]
41. Godfrey DI, Stankovic S, Baxter AG. Raising the NKT cell family. Nat Immunol. 2010; 11:197–206. [PubMed: 20139988]
42. Pereira P, Boucontet L. Innate NKTγδ and NKTαβ cells exert similar functions and compete for a thymic niche. Eur. J. Immunol. 2012; 42:1272–1281. [PubMed: 22539299]
43. Kovalovsky D, Alonzo ES, Uche OU, Eidson M, Nichols KE, Sant'Angelo DB. PLZF Induces the Spontaneous Acquisition of Memory/Effector Functions in T Cells Independently of NKT Cell-Related Signals. J. Immunol. 2010; 184:6746–6755. [PubMed: 20495068]
44. Matsuda JL, Zhang Q, Ndonye R, Richardson SK, Howell AR, Gapin L. T-bet concomitantly controls migration, survival, and effector functions during the development of Valpha14i NKT cells. Blood. 2006; 107:2797–2805. [PubMed: 16357323]
45. Iwabuchi K, Iwabuchi C, Tone S, Itoh D, Tosa N, Negishi I, Ogasawara K, Uede T, Onoé K. Defective development of NK1.1+ T-cell antigen receptor alphabeta+ cells in zeta-associated protein 70 null mice with an accumulation of NK1.1+ CD3- NK-like cells in the thymus. Blood. 2001; 97:1765–1775. [PubMed: 11238119]
46. Jensen KDC, Su X, Shin S, Li L, Youssef S, Yamasaki S, Steinman L, Saito T, Locksley RM, Davis MM, Baumgarth N, Chien Y-H. Thymic Selection Determines γδ T Cell Effector Fate: Antigen-Naive Cells Make Interleukin-17 and Antigen-Experienced Cells Make Interferon γ. Immunity. 2008; 29:90–100. [PubMed: 18585064]
47. Odumade OA, Weinreich MA, Jameson SC, Hogquist KA. Kruppel-Like Factor 2 Regulates Trafficking and Homeostasis of T Cells. J. Immunol. 2010; 184:6060–6066. [PubMed: 20427763]
48. Ueda-Hayakawa I, Mahlios J, Zhuang Y. Id3 Restricts the Developmental Potential of Lineage during Thymopoiesis. J. Immunol. 2009; 182:5306–5316. [PubMed: 19380777]
49. Jordan MS, Smith JE, Burns JC, Austin J-ET, Nichols KE, Aschenbrenner AC, Koretzky GA. Complementation in trans of altered thymocyte development in mice expressing mutant forms of the adaptor molecule SLP76. Immunity. 2008; 28:359–369. [PubMed: 18342008]
50. Yuan J, Nguyen CK, Liu X, Kanellopoulou C, Muljo SA. Lin28b Reprograms Adult Bone Marrow Hematopoietic Progenitors to Mediate Fetal-Like Lymphopoiesis. Science. 2012; 335:1195–1200. [PubMed: 22345399]

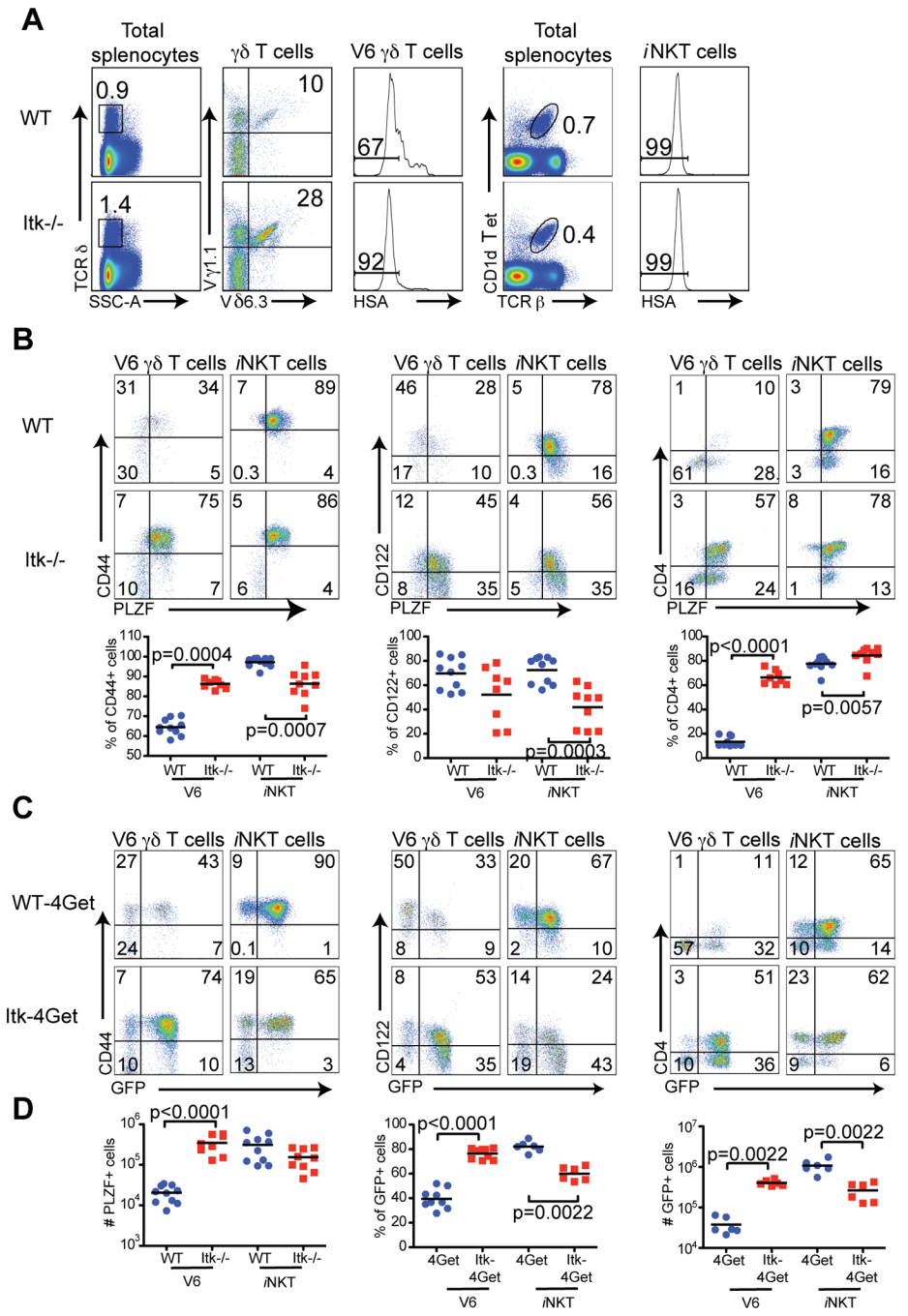

Figure 1. Splenic γδ NKT cells in *Itk*$^{-/-}$ mice have increased expression of PLZF and IL-4 mRNA

Splenocytes from WT and *Itk*$^{-/-}$ mice, or WT-4Get and *Itk*$^{-/-}$-4Get mice were stained and analyzed by flow cytometry.

(A) Total splenocytes were analyzed for TCRδ (left panels), and positive cells were gated on and examined for Vγ1.1 and Vδ6.3 expression (second panels). V6 cells were further examined for HSA expression (third panels). *i*NKT cells were identified by staining with CD1d tetramer and anti-TCR (fourth panels). *i*NKT cells further examined for HSA expression (right panels).

(B) HSA^- V6 γδ T cells and *i*NKT cells in the spleen were analyzed for expression of CD44, CD122, CD4 and intracellular PLZF. The mean fluorescent intensity of total PLZF in V6 cells is 395±41 for WT and 733±24 for $Itk^{-/-}$. Dot-plots show representative data; compilations of data from of all experiments are shown in the graphs below. Each data point represents one mouse and the black bars indicate the means. Statistically significant differences are shown with p values.
(C) HSA^- V6 γδ T cells and *i*NKT cells from WT-4Get and $Itk^{-/-}$-4Get mice were stained and analyzed for CD44 vs GFP, CD122 vs GFP and CD4 vs GFP expression. Data are representative of at least two independent experiments.
(D) Compilations of data show absolute numbers of $PLZF^+$ cells, and percentages and absolute numbers of GFP^+ cells within the HSA^- V6 γδ T cell or *i*NKT cell population. Statistically significant differences are shown with p values.

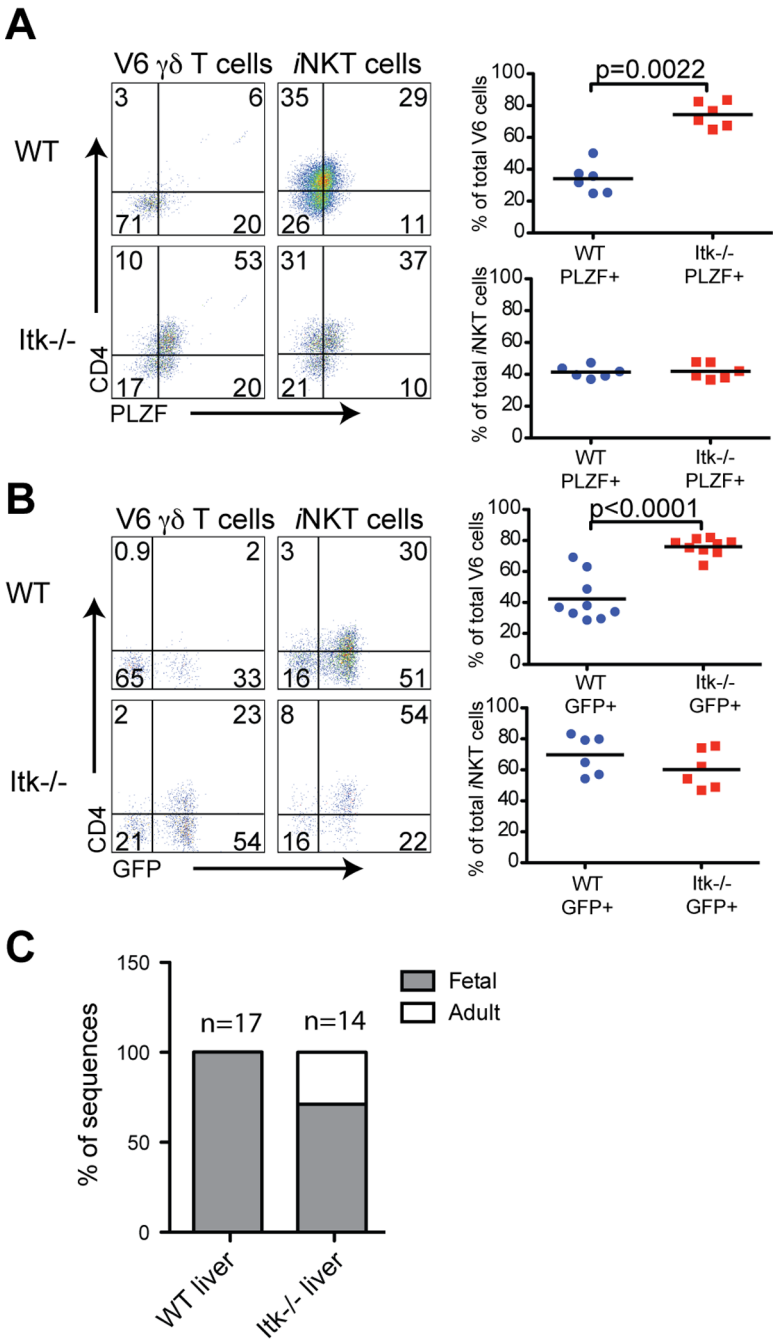

Figure 2. γδ NKT cells in the livers of *Itk*$^{-/-}$ have increased PLZF and IL-4 mRNA expression

Lymphocytes were isolated from livers of WT and *Itk*$^{-/-}$ mice or WT-4Get and *Itk*$^{-/-}$-4Get mice and were analyzed by flow cytometry.

(A) WT and *Itk*$^{-/-}$ HSA^{-} V6 γδ T cells and *i*NKT cells were examined for CD4 versus PLZF expression. Dot-plots show representative data, and the graphs show a compilation of data from all experiments. Statistically significant differences are shown with p values.

(B) WT-4Get and *Itk*$^{-/-}$-4Get HSA^{-} V6 γδ T cells and *i*NKT cells were analyzed for expression of CD4 and GFP. Dot-plots show representative data, and the graphs show compilations of data from all experiments. Statistically significant differences are shown with p values.

(C) Sorted V6 γδ T cells from WT and *Itk*$^{-/-}$ livers were analyzed for in-frame sequences of Vδ6 and Jδ1 junctions. The graph indicates the percentage of sequences corresponding to fetal-derived rearrangements or adult-derived rearrangements. The total number of sequences included in the analysis is indicated above each bar. Actual sequences are shown in Figure S1.

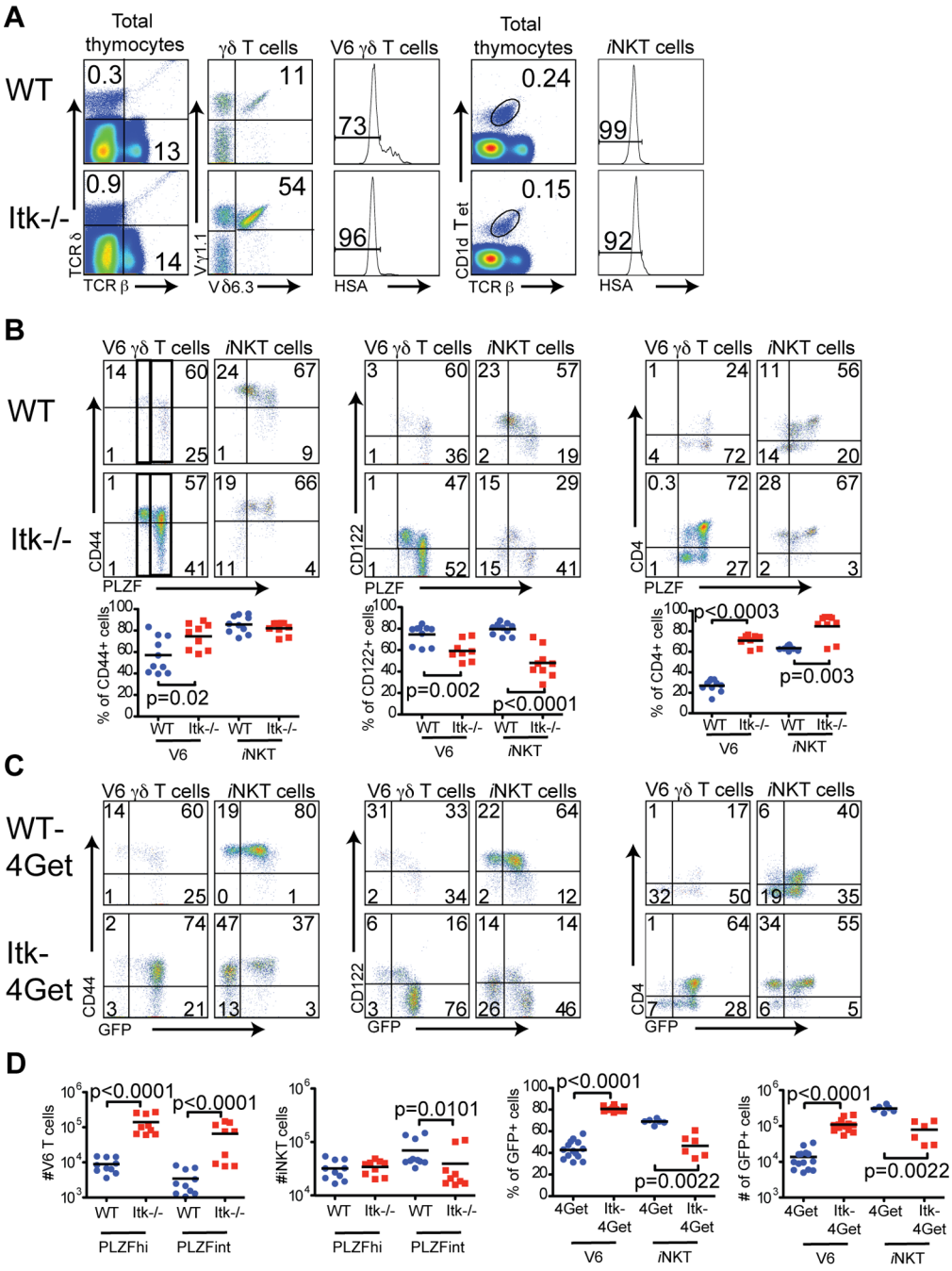

Figure 3. γδ NKT cells in the thymus of *Itk*$^{-/-}$ mice have characteristics of less mature αβ *i*NKT cells

Thymocytes from WT and *Itk*$^{-/-}$ mice, or WT-4Get and *Itk*$^{-/-}$-4Get mice were stained and analyzed by flow cytometry.

(A) Total thymocytes were analyzed for TCR versus TCRδ (left panels), and TCRδ-positive cells were gated on and examined for Vγ1.1 and Vδ6.3 expression (second panels). V6 cells were further gated on HSA (third panels). *i*NKT cells were identified by staining with CD1d tetramer and anti-TCR² (fourth panels). *i*NKT cells were further gated on HSA expression (right panels).

(B) HSA^- V6 γδ T cells and *i*NKT cells in the thymus were analyzed for expression of CD44, CD122, CD4 and intracellular PLZF. Dot-plots show representative data; compilations of data from of all experiments are shown in the graphs below. Statistically significant differences are shown with p values.
(C) HSA^- V6 γδ T cells and *i*NKT cells from WT-4Get and *Itk*$^{-/-}$-4Get mice were stained and analyzed for CD44 vs GFP, CD122 vs GFP and CD4 vs GFP expression. Data are representative of at least two independent experiments.
(D) $PLZF^{hi}$ and $PLZF^{int}$ V6 γδ T cell and *i*NKT cell populations were gated as shown in panel B and absolute numbers were calculated (left two panels). The percentages and absolute numbers of GFP^+ cells in the HSA^- V6 γδ T cell and *i*NKT cell populations are shown (right two panels). Statistically significant differences are shown with p values.

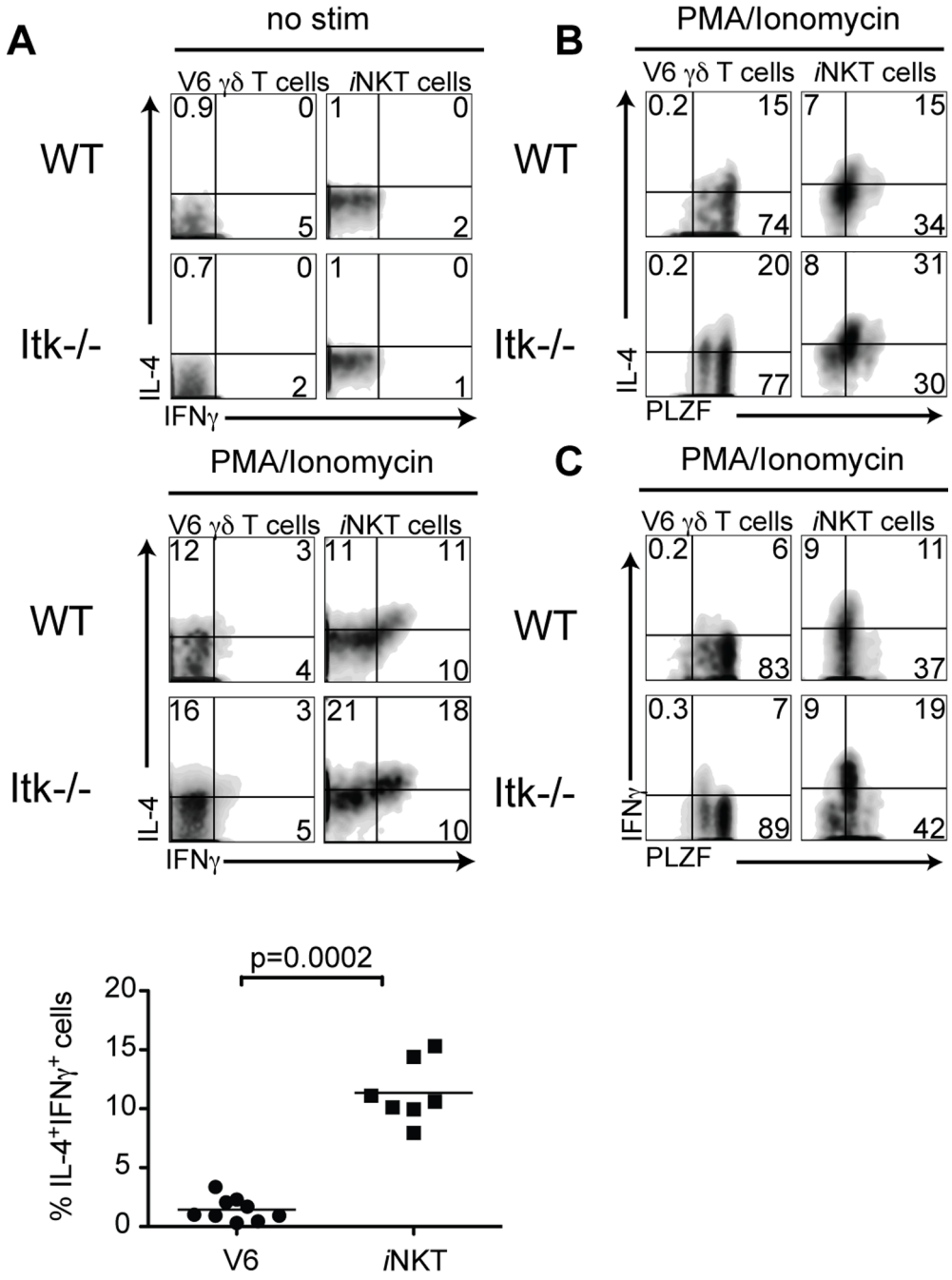

Figure 4. Levels of PLZF expression correlate with IFNγ production by γδ NKT cells

Thymocytes from WT or *Itk*$^{-/-}$ mice were stimulated with10ng/ml PMA and 2 μg/ml Ionomycin for 5 hours, and then stained for intracellular IL-4, IFNγ and PLZF. Dot-plots show gated HSA^{-} V6 thymocytes or CD1d tetramer positive cells.

(A) Non-stimulated (top) and stimulated (middle) cells were analyzed for IFNγ versus IL-4 production. The graph (bottom) shows a compilation of data indicating the percentage of double IL-4^{+} IFNγ^{+}-producing cells among WT V6 compared to *i*NKT cells. Statistical significance is shown with p value.

(B, C) Stimulated cells were analyzed for IL-4 versus PLZF expression (B) or IFNγ versus PLZF expression (C).

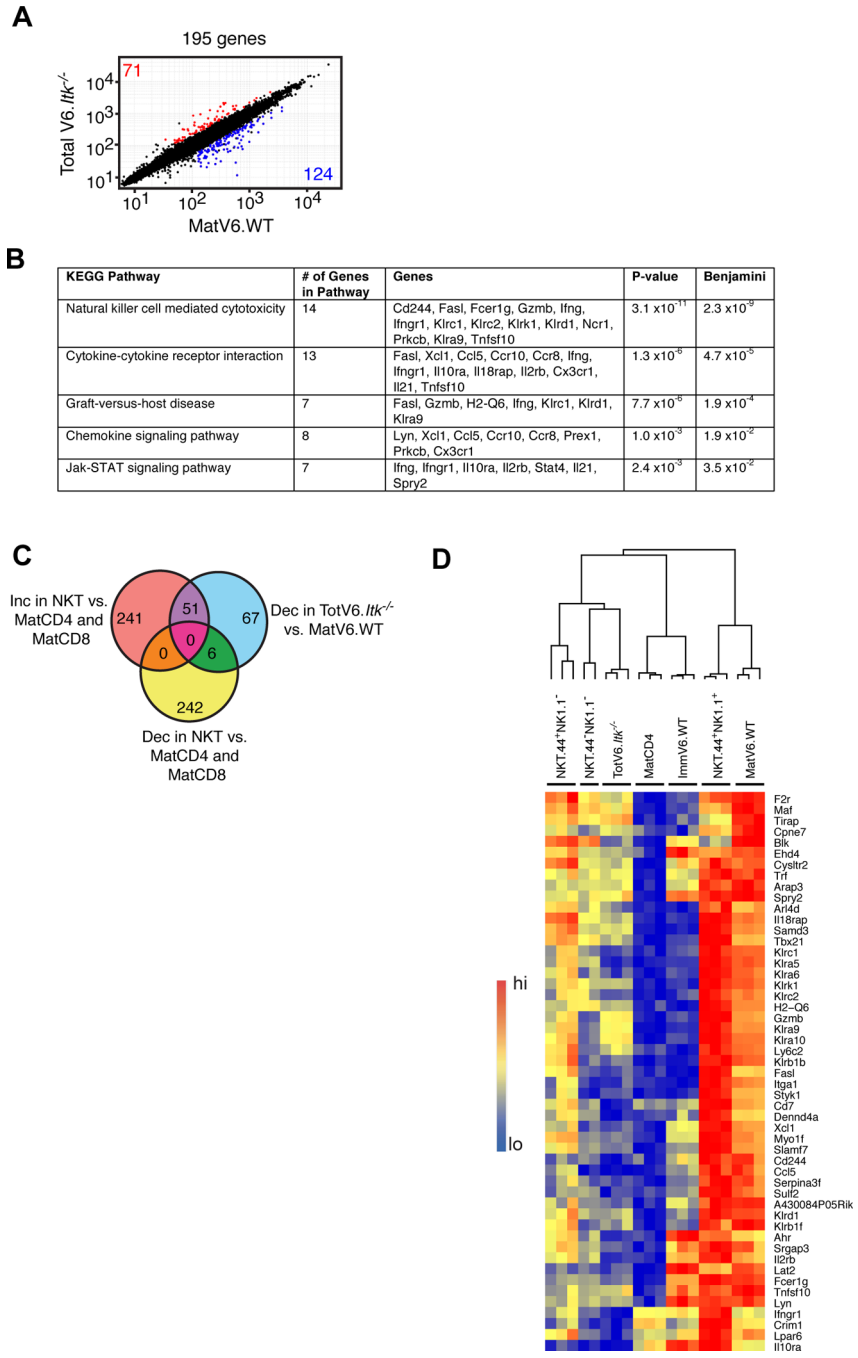

KEGG Pathway	# of Genes in Pathway	Genes	P-value	Benjamini
Natural killer cell mediated cytotoxicity	14	Cd244, Fasl, Fcer1g, Gzmb, Ifng, Ifngr1, Klrc1, Klrc2, Klrk1, Klrd1, Ncr1, Prkcb, Klra9, Tnfsf10	3.1×10^{-11}	2.3×10^{-9}
Cytokine-cytokine receptor interaction	13	Fasl, Xcl1, Ccl5, Ccr10, Ccr8, Ifng, Ifngr1, Il10ra, Il18rap, Il2rb, Cx3cr1, Il21, Tnfsf10	1.3×10^{-6}	4.7×10^{-5}
Graft-versus-host disease	7	Fasl, Gzmb, H2-Q6, Ifng, Klrc1, Klrd1, Klra9	7.7×10^{-6}	1.9×10^{-4}
Chemokine signaling pathway	8	Lyn, Xcl1, Ccl5, Ccr10, Ccr8, Prex1, Prkcb, Cx3cr1	1.0×10^{-3}	1.9×10^{-2}
Jak-STAT signaling pathway	7	Ifng, Ifngr1, Il10ra, Il2rb, Stat4, Il21, Spry2	2.4×10^{-3}	3.5×10^{-2}

Figure 5. Gene expression microarray analysis indicates impaired terminal maturation of *Itk*$^{-/-}$ γδ NKT cells

(A) Scatter plot showing expression of consolidated probe sets by CD24(HSA)^{lo} V6 γδ T cells in thymocytes from adult WT and *Itk*$^{-/-}$ mice. Nomenclature is according to ImmGen (immgen.org): MatV6.WT= CD24(HSA)^{lo} V6 γδ T cells from adult WT thymus; TotalV6.Itk$^{-/-}$, total V6 γδ T cells from adult *Itk*$^{-/-}$ thymus, which are 95–98% CD24^{lo}. Each dot represents one gene (mean of all probe sets and mean of replicates); red and blue indicate genes with expression increased or decreased, respectively, by more than twofold ($P < 0.05$ (Student's *t*-test); coefficient of variation < 0.5; mean expression value (MEV) > 120 in one subset); numbers in parentheses above plot indicates total number of these genes. The

numbers within the plot indicate the number of up-regulated (red) or down-regulated (blue) genes in the comparison. Data are from three independent experiments with 4–30 mice each.
(B) The 124 genes increased in MatV6.WT versus TotalV6.Itk$^{-/-}$ cells were classified into functional pathways using the KEGG analysis program (DAVID). The top five pathways enriched in the dataset are shown along with the number of genes, the gene names, the *P*-value, and the Benjamini *P*-value for each pathway.
(C) Venn diagram comparing the list of genes that were increased or decreased in *i*NKT (NKT.44^{+}NK1.1^{+}) cells versus MatCD4 (CD24^{lo}) and MatCD8 (CD24^{lo}) single positive thymocytes (identified previously in (21)) with the list of 124 genes down-regulated in TotalV6.Itk$^{-/-}$ versus MatV6.WT cells. Roughly 40% of the genes decreased in TotalV6.Itk$^{-/-}$ versus MatV6.WT cells are normally increased in NKT.44^{+}NK1.1^{+} cells versus mature single-positives.
(D) Heat map showing relative expression of the 51 genes identified in Figure 5C that were decreased in TotalV6.*Itk*$^{-/-}$ versus MatV6.WT cells and increased in NKT.44^{+}NK1.1^{+} cells versus MatCD4 and MatCD8 single positive thymoctyes in populations of NKT and MatCD4 cells from WT mice and V6 cells from WT or *Itk*$^{-/-}$ mice. Data were log transformed, centered by gene row and hierarchically clustered by gene and subset. The clustering dendrogram for samples is shown. Color coding reflects relative expression levels of a given gene in each subset, and does not provide information about absolute expression levels of each gene.

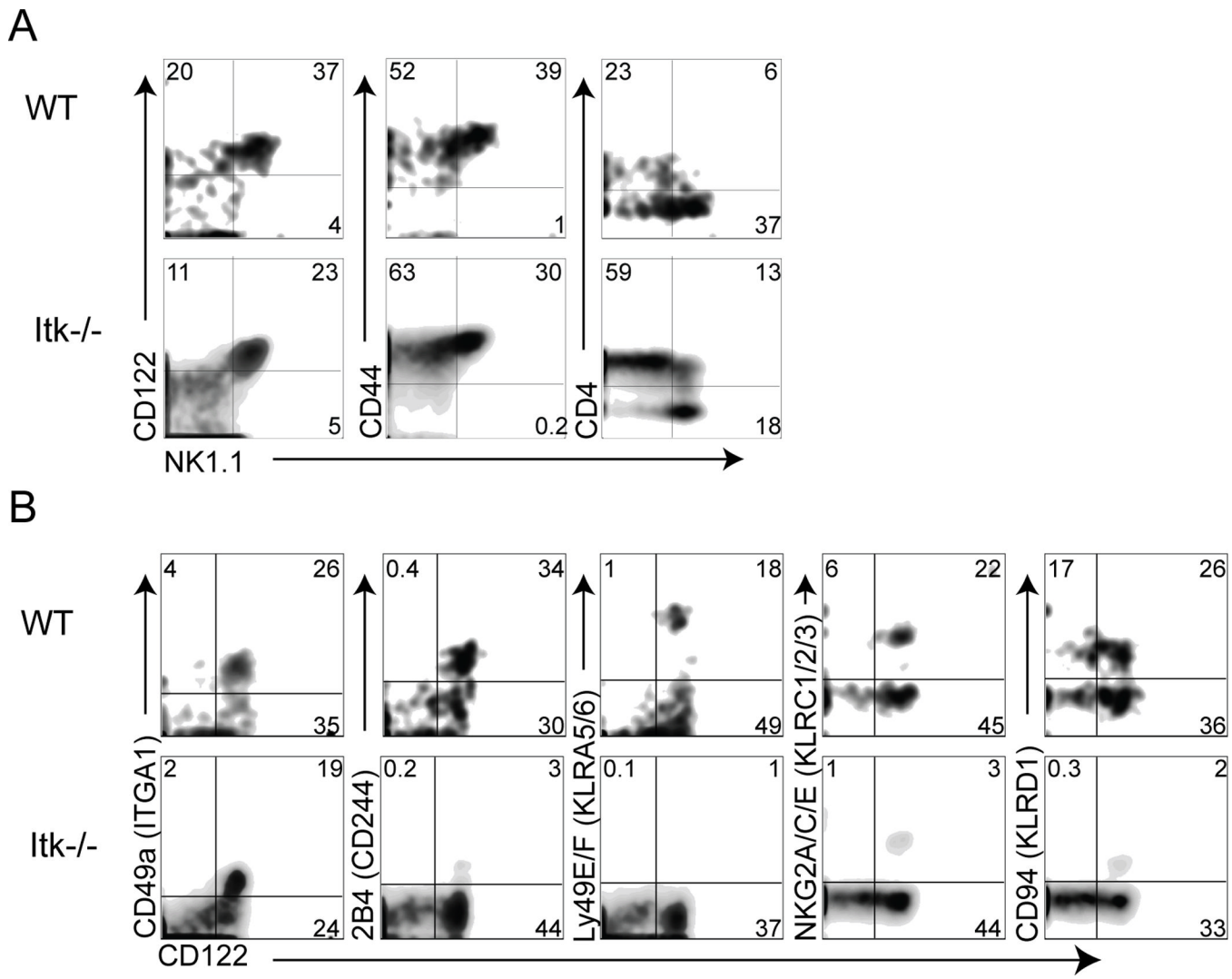

Figure 6. Decreased surface expression of NK cell markers on *Itk*$^{-/-}$ V6 cells

(A) Thymocytes from WT and *Itk*$^{-/-}$ mice were stained for expression of NK1.1 along with CD122, CD44 and CD4. (B) Thymocytes from WT and *Itk*$^{-/-}$ mice were stained for expression of NK cell markers CD49a (ITGA1), 2B4 (CD244), Ly49E/F (KLRA5/6), NKG2A/C/E (KLRC1/2/3), CD94 (KLRD1) and CD122. Dot-plots show gated CD24^{lo} V6^{+} cells. Results are representative of 2 experiments with at least 3 mice per group.

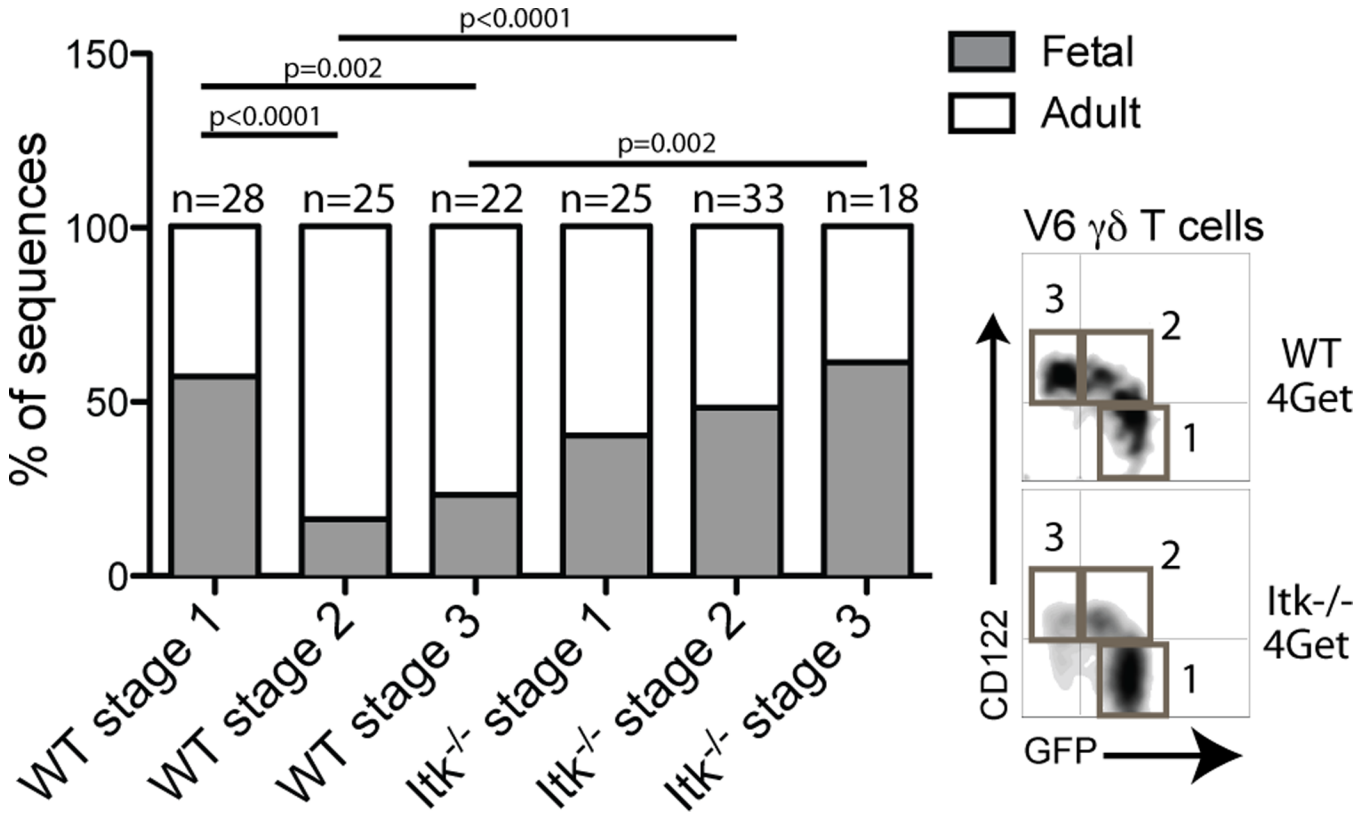

Figure 7. The expanded population of γδ NKT cells in the thymus of *Itk*$^{-/-}$ mice include cells derived from both fetal and adult progenitors

The graph shows the relative proportions of in-frame TCR Vδ6 and Jδ1 junctions in three subsets of sorted thymocytes from WT-4Get and *Itk*$^{-/-}$-4Get mice that derive from fetal versus adult progenitors. Populations analyzed were: CD122^{-}GFP^{+} (Stage 1), CD122^{+}GFP^{+} (Stage 2), and CD122^{+}GFP^{-} (Stage 3). The total number of sequences included in the analysis is indicated above each bar. Statistically significant differences were determined using the exact binomial test of goodness-of-fit, and p values are shown. At the right, the gating strategy for isolation of each thymocyte subset is shown.

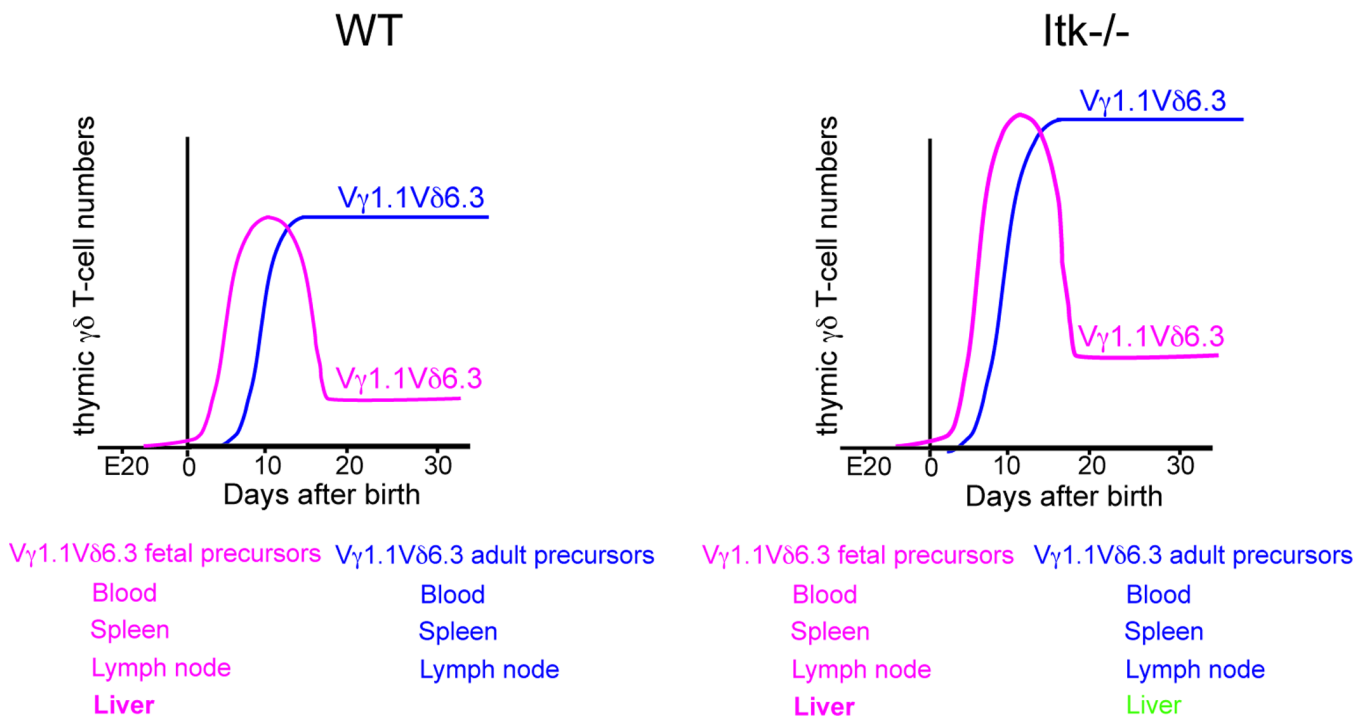

Figure 8. A model of V6 development in wild type and *Itk*$^{-/-}$ mice

In wild-type (WT) mice (left), V6 cells initially develop from fetal precursors (pink) and expand in the thymus during the first two weeks after birth (22). These cells undergo a maturation program similar to αβ iNKT cells before emigrating to the periphery, with a preference for homing to the liver (bold pink). As WT mice age, a second wave of V6 cells develops from adult precursors (blue) and matures prior to emigrating to peripheral lymphoid organs. A small number of fetal-derived and adult-derived V6 cells are present and continuously maturing in the thymus of adult mice. Similar to WT V6 cells, *Itk*$^{-/-}$ V6 cells (right) also initially develop from fetal precursors (pink) and preferentially home to the liver; however increased numbers of V6 cells are found in the absence of Itk. A second wave of adult precursor-derived *Itk*$^{-/-}$ V6 cells also develops in increased numbers (blue). *Itk*$^{-/-}$ V6 cells have a defect in terminal maturation and retain high expression of PLZF and IL-4 relative to WT V6 cells. In addition, *Itk*$^{-/-}$ V6 cells arising from adult precursors are able to emigrate to the liver (green). E20, embryonic day 20.